Journal of Bioenergetics and Biomembranes, Vol. 32, No. 4, 2000

The *b* Subunit of *Escherichia coli* ATP Synthase

Stanley D. Dunn,[1,2] Matthew Revington,[1] Daniel J. Cipriano,[1] and Brian H. Shilton[1]

The *b* subunit of ATP synthase is a major component of the second stalk connecting the F_1 and F_0 sectors of the enzyme and is essential for normal assembly and function. The 156-residue *b* subunit of the *Escherichia coli* ATP synthase has been investigated extensively through mutagenesis, deletion analysis, and biophysical characterization. The two copies of *b* exist as a highly extended, helical dimer extending from the membrane to near the top of F_1, where they interact with the δ subunit. The sequence has been divided into four domains: the N-terminal membrane-spanning domain, the tether domain, the dimerization domain, and the C-terminal δ-binding domain. The dimerization domain, contained within residues 60–122, has many properties of a coiled-coil, while the δ-binding domain is more globular. Sites of crosslinking between *b* and the *a*, α, β, and δ subunits of ATP synthase have been identified, and the functional significance of these interactions is under investigation. The *b* dimer may serve as an elastic element during rotational catalysis in the enzyme, but also directly influences the catalytic sites, suggesting a more active role in coupling.

KEY WORDS: ATP synthase; second stalk; *b* subunit; stator; rotational catalysis; coiled-coil.

INTRODUCTION

The synthesis of ATP in the processes of oxidative phosphorylation and photophosphorylation is catalyzed by ATP synthase, an enzyme found in the cytoplasmic membranes of bacteria, the thylakoid membranes of chloroplasts, and the inner membranes of mitochondria. This enzyme consists of two sectors, the membrane-integral F_0, which catalyzes the movement of protons across the membrane, and the membrane-peripheral F_1-ATPase, which catalyzes the synthesis or hydrolysis of ATP. The F_1 of the prototypical ATP synthase from *Escherichia coli* consists of five different polypeptide chains in a stoichiometry of $\alpha_3\beta_3\gamma\delta\varepsilon$; the F_0 from this bacterium is composed of three subunits in a stoichiometry of ab_2c_{10-12}. In addition to other articles within this issue, a number of reviews stressing various aspects of ATP synthase structure and function have been published recently (Boyer, 1997; Weber and Senior, 1997; Nakamoto *et al.*, 1999; Walker, 2000).

Catalytic sites for nucleotides are located primarily on β subunits with minor contributions from adjacent α subunits, while residues critical for proton translocation reside on the *a* and *c* subunits. Both ATP synthesis and ATP-dependent proton pumping depend on coupling the two catalytic activities; this coupling requires the γ, δ, ε, and *b* subunits. Before the mechanism of coupling can be discussed, the overall structure of the enzyme should be considered in greater detail. No high-resolution structure of the entire enzyme is available; a subunit model based on crystal structures of bovine mitochondrial F_1 (Abrahams *et al.*, 1994), an $\alpha_3\beta_3\gamma\varepsilon c_{10}$ assembly of yeast mitochondria (Stock *et al.*, 1999), individual subunit or domain structures (Wilkens *et al.*, 1995, 1997; Girvin *et al.*, 1998; Uhlin *et al.*, 1997) electron microscopy (Wilkens *et al.*, 2000), and other data is presented in Fig. 1. The three α and β subunits form an alternating hexagonal array with an elongated cavity in the middle and a dimple at the top. Most of the cavity is occupied by an asym-

[1] Department of Biochemistry, University of Western Ontario, London, Ontario N6A 5C1, Canada.
[2] To whom correspondence should be addressed: e-mail: sdunn@julian.uwo.ca

0145-479X/00/0800-0347$18.00/0

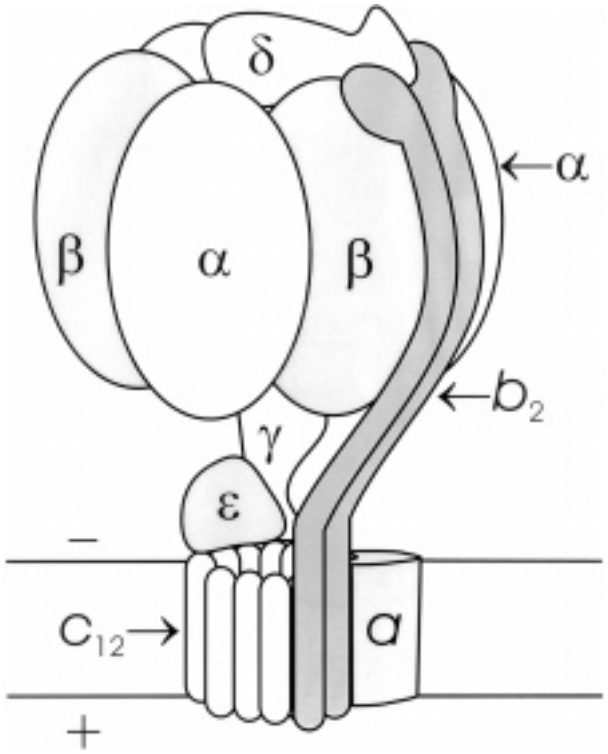

Fig. 1. Subunit model of *E. coli* ATP synthase. The model is a composite incorporating information from crystal structures, NMR structures, electron microscopy, cross-linking analysis, and other forms of protein structural analysis.

metric antiparallel coiled-coil formed by the N-and C-terminal segments of γ, while the rest of γ is located near the membrane and binds ε, forming the larger, more central, stalk. The multiple *c* subunits are embedded in the membrane as a ring with lipid in the center; the γ and ϵ subunits contact a limited number of *c* subunits through the polar loop regions of the latter. Subunit *a* is mostly embedded in the membrane and interacts with the outside of the *c* ring. Subunit *b* has an N-terminal membrane anchor, located close to the *a* subunit, but the balance of the polypeptide is highly polar. The two copies of *b* exist as a dimer reaching from the membrane nearly to the top of F_1 where they interact with the C-terminal part of δ to complete the second, or peripheral, stalk. The N-terminal part of δ sits in the dimple at the top of F_1.

The synthesis of ATP is believed to depend on the rotational motion of the $\gamma\varepsilon c_{12}$ complex, sometimes called the rotor, relative to $\alpha_3\beta_3\delta a b_2$. According to the current consensus model, proton movement through F_0 is thought to drive rotation of the *c* oligomer past the *a* subunit, one proton crossing the membrane as each *c* subunit passes critical residues on *a*. Energy is transferred to F_1 through the coupled rotation of γε, with the intrinsic asymmetry of the γ coiled-coil inside the $\alpha_3\beta_3$ hexamer causing conformational changes in the β subunits. These conformational changes result in the binding of ADP + P_i and the release of ATP from catalytic sites, with all three β subunits participating sequentially. The changes in binding properties, rather than the chemical synthesis of ATP, is the major endergonic step of ATP synthesis (Boyer, 1997). In this model the primary function of the second stalk is to serve as a stator, preventing $\alpha_3\beta_3$ from rotating with γε, so that the conformational changes can be effected.

Since we reviewed the second stalk of the *E. coli* enzyme just over a year ago (Dunn *et al.*, 2000b), the present review will focus on recent progress on the *b* subunit. The sequence of this 156-residue, 17,264-Da polypeptide (Fig. 2) reveals the existence to two distinct regions, a hydrophobic N-terminal transmembrane domain and a larger, more polar, remainder. This pattern is characteristic of *b*-type subunits, although mitochondrial *b* has two consecutive membrane-spanning segments at the N-terminus.

THE POLAR REGIONS OF *b* SUBUNITS

The expressed polar region of *E. coli b* exists in solution as a highly extended dimer capable of binding to F_1-ATPase (Dunn, 1992). Because of its high degree of extension, attempts to determine the solution molecular weight of *b* by techniques dependant on shape give notably erroneous values. For instance, $b_{25–156}$ (originally called b_{sol}) elutes from a calibrated size exclusion column with an apparent molecular weight of 85,000. The shape-independent technique of sedimentation equilibrium ultracentrifugation, in which a stable distribution of protein is generated at a low rotor speed, gives a more reliable value of around 30,000, consistent with a dimer of 15.5-kDa monomers. The shape of the dimer was studied by a different type of ultracentrifuge experiment, called sedimentation velocity ultracentrifugation, in which the rate of sedimentation of the protein at a high rotor speed is measured. This rate depends on both the mass and the shape of the protein; knowing the molecular weight to be about 31,000 and the sedimentation coefficient to be 1.8 *S*, allows one to calculate that the $b_{25–156}$ dimer has a frictional coefficient 1.9-fold higher than expected for a smooth sphere of the same mass and density. This high frictional ratio indicates that the

dimer is notably extended in shape, but cannot reveal details of the structure. Circular dichroism (CD) spectroscopy has shown b_{25-156} to be greater than 60% helical. More recently, it was shown that the dimerization was not very strong, that monomer and dimer exist in a dynamic equilibrium, and that dimer can be largely converted to monomer at 40°C, the maximal operating temperature of the Beckman XL-A analytical ultracentrifuge (Revington *et al.*, 1999). A related melting has also been observed using the CD signal (Rodgers *et al.*, 1997). Recently, the entire *b* subunit was purified by SDS-PAGE, reconstituted into liposomes, and analyzed by CD spectroscopy (Greie *et al.*, 2000). These workers concluded that the subunit was about 80% helix, with most of the remainder in the form of turn or extended conformation. Overall, these results supported the predominantly helical nature of the polar domain of the subunit but do not reveal which segments are helical, and which are not.

Photosynthetic organisms encode two *b*-type subunits, called *b* and *b′*. Recently, in collaboration with Holger Lill's laboratory, the polar regions of the *b* and *b′* subunits from the cyanobacterium *Synechocystis* PCC6803 were expressed and examined by similar techniques (Dunn *et al.*, manuscript submitted). Each of these polypeptides existed individually as a monomer, with helical content on the order of 40 to 50%. When they were mixed, formation of heterodimers could be observed by either chemical crosslinking or sedimentation equilibrium analytical ultracentrifugation. An increase in helicity, up to at about 60%, was also observed. The heterodimer had a frictional ratio of 2.1 and melted at 40°C. Overall, these results imply that *b* and *b′* exist in the ATP synthases of photosynthetic organisms in a heterodimeric form and the similarity of properties of this heterodimer to the soluble *b* homodimer of *E. coli* implies that the latter is a good model for *b* subunits from other eubacteria and photosynthetic organisms.

THE DOMAIN STRUCTURE OF *E. coli b*

Unfortunately, as yet, no high-resolution structure of most of the *b* subunit is available, either in isolation or as a part of ATP synthase. The membrane-spanning domain present in residues 1–34 has been solved by NMR (Dmitriev *et al.*, 1999), revealing a helical structure with a bend at residues 23–26. However, the polar region has been refractory to both crystallographic and NMR analysis. Crystals of the entire polar domain have been obtained (Dunn *et al.*, 2000b), but in no cases did they diffract X-rays well enough to warrant analysis. NMR spectra have shown very little dispersion. The problems afflicting both of the methods of determining protein structures at high resolution have their roots in the nature of the polar domain of *b*. It is extended rather than globular, highly helical, its dimerization is relatively weak and reversible, and it exhibits evidence of flexibility. All of these factors serve to make structural analysis a challenge.

We have, therefore, pursued additional approaches to gain structural knowledge of the *b* dimer. Hydrodynamic analysis of deletion constructs has led to development of a four-domain model as illustrated in Fig. 2 and additional information has been provided by spectroscopic and protein chemical approaches.

Beginning with b_{24-156}, the entire polar region, we determined how many residues could be removed from each end without a major effect on dimerization,

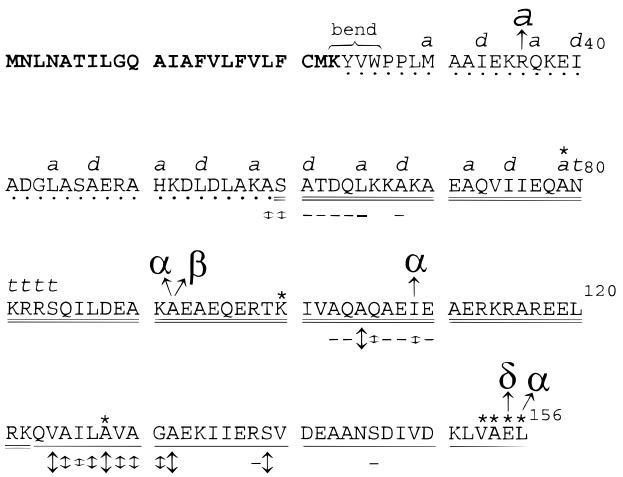

Fig. 2. Amino acid sequence of the *E. coli b* subunit. The amino acid sequence, domain structure, and residues of known significance are shown. The transmembrane domain is indicated by boldface, the tether domain by the dotted underline, the dimerization domain by the double underline, and the δ-binding domain by the single underline. A number of features are indicated above the sequence. A rigid bend was observed at positions 23–26 in the NMR structure of residues 1–34. The *a* and *d* positions of the heptad repeat between positions 30 and 79 are noted and residues 80–84, which are predicted to form a turn, are indicated by *t*. Positions that have been crosslinked to other subunits of ATP synthase are indicated by the single-headed arrows. Mutation or deletion of residues marked by asterisks leads to structural disruption of the local domain. The tendency of introduced cysteine residues to form intersubunit disulfides in the soluble *b* constructs is indicated below the sequence, with the size of the double-headed arrows indicating the relative tendency toward disulfide formation. The straight bars indicate little or no tendency toward disulfide formation.

as measured in the ultracentrifuge. From this we learned that the region essential for dimerization is contained within the sequence from Asp53 to Lys122 (Revington *et al.*, 1999), and more recent studies show that we can move the N-terminal boundary of this dimerization domain to at least Ser60 (Dunn, unpublished observations). Residues between the membrane domain and the dimerization domain form the tether domain, which links the two definable regions. The C-terminal region, from residue Gln123 to the C-terminus Leu156, forms a more globular structure that serves to bind δ.

THE TETHER DOMAIN

The tether domain, between residue 25 and approximately residue 60, is the least defined part of the *b* subunit. A heptad repeat, extending from just outside the membrane and continuing without interruption to residue Ala79 (Dunn, 1992; McCormick *et al.*, 1993), suggests a coiled-coil arrangement. If this structure does exist in the tether domain, it contributes little to the stability of dimerization.

A most remarkable feature of this part of the *b* sequence is its ability to accommodate the deletion of up to 11 residues, and still assemble into functional ATP synthase *in vivo*, provided the mutant subunit is overexpressed (Sorgen *et al.*, 1998b). The residues deleted in these constructs were mostly in the C-terminal end of the tether domain and the N-terminal end of the dimerization domain. Since then, the work has been extended to demonstrate that insertions of up to 14 residues in the same region are tolerated (Sorgen *et al.*, 1999). Given the role of $b_2\delta$ in reaching from the membrane to the top of F_1, one would have expected the deletions to be too short and the insertions too long. The fact that enzyme containing these alterations can function suggests that some part of the $b_2\delta$ complex must be flexible or elastic so that it can stretch or take up the slack. This conclusion leaves an open question of why, despite the low conservation of individual amino acid residues in *b*, gaps are seldom found when multiple *b* sequences are aligned (Blair *et al.*, 1996; Tiburzy and Berzborn, 1997). It should be noted in this regard that a recent revision to the sequence of the *b* subunit of the alkalophile *Bacillus firmus* (SWISS-PROT Acc. No. P22481) has brought this sequence into better alignment with other *b* sequences.

Among the few residues in *b* that are conserved through evolution is Arg36 and mutagenesis of this site caused both lower levels of assembly and functional defects, including uncoupling (Caviston *et al.*, 1998). More recently, we have shown that a cysteine substituted into position 36 can be crosslinked to the *a* subunit of F_0 (McLachlin *et al.*, 2000). The proximity of this conserved position to subunit *a* suggests that it may participate in signaling events between the two catalytic regions of the enzyme.

THE DIMERIZATION DOMAIN

The C-terminal boundary of the dimerization domain was established by the findings that truncation from the C-terminus back to residue Lys122 had no major effect on dimerization, but cutting it back to residue Lys114 resulted in monomeric protein (Revington *et al.*, 1999). Finally, the $b_{53–122}$ form of the protein was constructed and shown to be dimeric. In thermal denaturation studies, $b_{53–122}$ melts with characteristics similar to those of the entire domain, suggesting that the most relevant intersubunit contacts are within the region (Revington *et al.*, 2000).

Our result that truncation of *b* back to position 122 had little effect on dimerization might be seen as conflicting with the result previously published by another laboratory that the mutation of residue Ala128 to aspartic acid caused *b* to become monomeric (Howitt *et al.*, 1996). A re-examination of the impact of this mutation on the structure and interactions of *b* within the context of $b_{34–156}$ showed no significant effect of the mutation on the dimerization of the construct, as measured by sedimentation equilibrium ultracentrifugation (Dunn *et al.*, 2000a). The reason for the discrepancy between our results and those of Howitt *et al.* (1996) is not obvious. We did find that the mutation caused a conformational change in the C-terminal region accompanied by the loss of ability to bind F_1-ATPase (see section on "The δ-Binding Domain").

A number of lines of evidence point to the dimerization domain having substantial coiled-coil content. First, the shape of $b_{53–122}$, as determined both from its frictional coefficient in the ultracentrifuge and from NMR relaxation parameters, is consistent with a coiled-coil of the expected length (Revington *et al.*, 1999). Second, small-angle X-ray scattering by the polypeptide in solution indicates a maximum dimension of the dimeric domain to be 100–110 Å, again consistent with helices of the expected length (Shilton *et al.*, unpublished observations). Third, the CD spectrum of the domain indicates close to 100% helix at 5 or 20°C and is indicative of coiled-coil structure, in that the minimum at 222 nm has an intensity similar

to that of the minimum at 208 nm (Revington *et al.*, in preparation). This spectral property is characteristic of coiled-coils, whereas spectra of globular proteins with noninteracting helices typically show minima at 222 nm that are 80–85% as intense as those at the shorter wavelength (Lau *et al.*, 1984). Fourth, analysis of the tendency toward disulfide formation of cysteines introduced at positions between Ala103 and Glu110 reveals a periodicity consistent with parallel interacting helices (Revington *et al.*, 1999). However, a similar analysis of residues between positions Ala59 and Ala68 failed to show this pattern, implying a less regular structure in the region near the junction of the tether and dimerization domains (McLachlin and Dunn, 1997).

The sequence from residues Asn80 to Ser84 is predicted to form a bend by secondary structure programs, but the actual structure of the region is unknown. Analysis of the $b_2\delta$ complex in the ultracentrifuge showed that the *b* dimer can bend at some unknown position (McLachlin *et al.*, 1998). Work in Brian Cain's laboratory (McCormick *et al.*, 1993; Sorgen *et al.*, 1998a) explored the importance of residue Ala79, which immediately precedes the predicted turn and is highly conserved among *b* subunit sequences. These workers found that the majority of the expressed polar domains containing substitutions to this site had a much reduced tendency to form dimers and that the ability to bind F_1 *in vitro* was well correlated with the potential for dimer formation. Growth on succinate, however, was significantly affected only by the most radical substitutions, such as glutamate, lysine or proline, at this position of the full-length *b* subunit. These results suggest that additional factors, such as the proximity imparted by the membrane anchors or possibly interactions with F_1 favor dimer formation *in vivo*.

Two new lines of evidence imply that the dimerization domain of *b* has a well-defined structure, with less tolerance for major changes than seen in the region of the junction with the tether domain. First, we have found that deletion of a single residue, Lys100, in the dimerization domain causes the loss of dimerization *in vitro* and the failure to grow on succinate *in vivo*, even when the protein is expressed at levels higher than normal (Cipriano and Dunn, unpublished observations). Second, we have obtained crystals of a dimerization domain construct, which diffract X-rays to better than 2.5 Å resolution using a rotating anode X-ray generator (Fig. 3; Shilton and Dunn, unpublished observations), indicating a high state of order and conformational homogeneity.

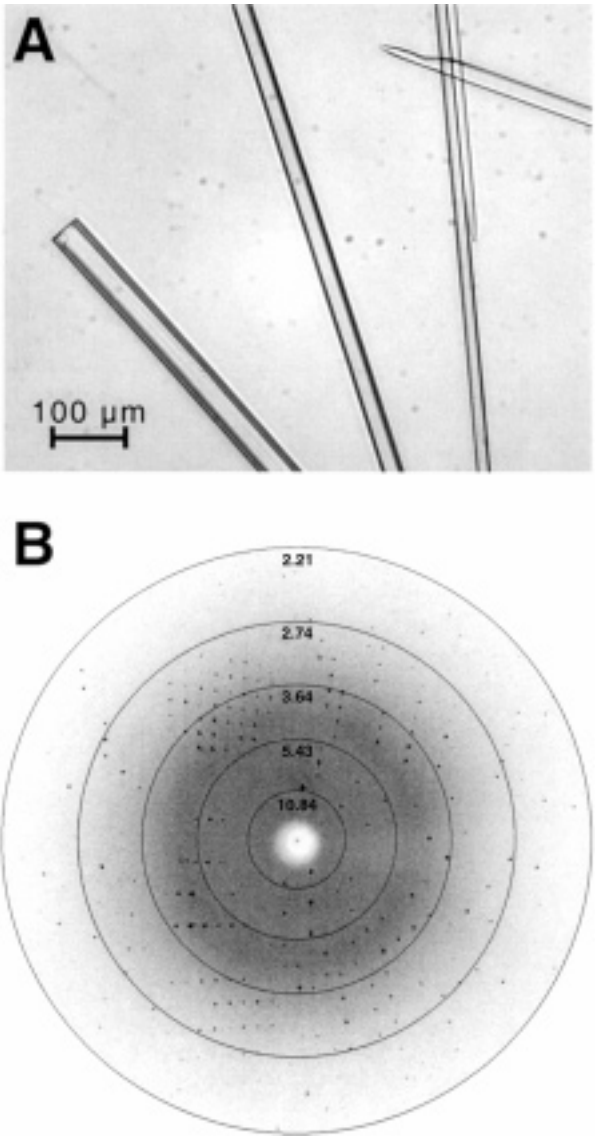

Fig. 3. Crystals of the dimerization domain of *E. coli b* subunit. Crystals of a dimerization domain construct were grown by the sitting-drop technique. Panel A illustrates crystals of the b_2 dimerization domain. The crystals are typically rod-shaped, over 1 mm long, and up to 100 μm in the two shorter dimensions. Panel B shows the diffraction pattern from a b_2 dimerization domain crystal, recorded at 100°K using a rotating anode source and image plate area detector. The rings correspond to Bragg spacings of 10.8, 5.4, 3.6, 2.7, and 2.2 Å. The protein crystallizes in space group $P2_12_12$ with unit cell dimensions $a = 35.5$, $b = 40.9$, and $c = 42.2$ Å.

THE δ-BINDING DOMAIN

In contrast to the tether domain, the C-terminal δ-binding domain has both a defined structure and a clear function. Work in Masamitsu Futai's lab a number of years ago showed that truncation of *b* by a few

residues caused defective assembly of ATP synthase (Takeyama *et al.*, 1988). Subsequent work from our laboratory revealed that the very C-terminal residues are essential for binding F_1 or δ and that the C-terminus of *b* can be chemically crosslinked to position Met158 of δ (McLachlin *et al.*, 1998). The role of the C-terminal region of mitochondrial *b* in binding oligomycin sensitivity-conferring protein (OSCP), the analog of *E. coli* δ, has been demonstrated through subunit interaction (Collinson *et al.*, 1994) and chemical crosslinking (Soubannier *et al.*, 1999) analyses.

Either the A128D mutation or the deletion of residues 153–156 from *b* cause the loss of δ-dependent interaction with F_1. The globular nature of the δ-binding region of *E. coli b* was revealed by the effects of either these mutations or cold temperature on the sedimentation coefficient, which depends on both shape and molecular weight. The sedimentation coefficients of a number of forms of *b*, all dimeric under the conditions employed, were measured at either 5 or 20°C, then corrected for density and viscosity to obtain the values of $s_{20,w}$ (Table I). Beginning with the data collected at 20°C, the complete polar domain, $b_{24–156}$, sedimented at 1.74 *S*, whereas $b_{24–152}$ sedimented at just 1.46 *S*. This decrease is far larger than would be expected from the small change in molecular weight, implying a conformational change in which the protein became more extended causing an increase in the frictional coefficient. As can be seen in the next two lines, the A128D mutation caused a similar change in the context of the $b_{34–156}$ construct (Dunn *et al.*, 2000a). Carrying out the studies at 5°C reduced the sedimentation coefficients of the wild-type sequences, but had little or no effect on the sedimentation coefficients of the truncated or mutant polypeptides. In fact, at the lower temperature, all samples showed very similar sedimentation coefficients. These results imply that either the mutations or the lower temperatures induce similar effects on the structure of the *b* dimer.

Table I. Effects of Temperature and Mutations to the C-Terminal Domain of *b* on the Sedimentation Coefficient of the Dimer

	$s_{20,w}(S)$	
Polypeptide	5°C	20°C
$b_{24–156}$	1.55 ± 0.01[a]	1.74 ± 0.04[a]
$b_{24–152}$	1.52 ± 0.00[a]	1.46 ± 0.02[a]
$b_{34–156}$	1.54 ± 0.02[b]	1.76 ± 0.01[b]
$b_{34–156}$A128D	1.51 ± 0.01[b]	1.54 ± 0.01[b]

[a] Data from Revington *et al.* (1999).
[b] Data from Dunn *et al.* (2000a).

The faster sedimentation of the normal *b* dimer at 20°C, and the location of the mutations, imply that the conformational change is one in which the C-terminal domain goes from a more folded or globular structure to a less folded and more extended state. How could each of these minor changes cause this unfolding? The C-terminal 10 residues have the potential to form an amphipathic helix (McLachlin *et al.*, 1998), so removal of the last four of these residues (VAEL) could disrupt interactions essential to the integrity of the domain. Residue 128 is on the side of the helices that appear to be nearest each other, so electrostatic repulsion could push the chains apart, causing a loss of interactions critical to maintaining the folded state. Finally, cold lability in proteins is normally ascribed to a weakening of the hydrophobic effect, suggesting the importance of nonpolar residues in the folding of this region. Another significant effect of the unfolding is a reduced tendency to aggregate to species higher than dimer. Overall, we infer that the C-terminal domain has a weakly folded structure in which hydrophobic residues are arranged so as to both impart stability to the structure and also to create one or more hydrophobic patches on the surface. The folded structure seems to be required for interaction with F_1 and the exposed hydrophobic patches are logical candidates for sites of this interaction.

THE INTERACTION OF *b* WITH F_1

Previously reviewed work has established the interaction of b_2 with δ, mediated by the C-terminal domains of each (Rodgers *et al.*, 1997; Sawada *et al.*, 1997; Dunn and Chandler, 1998; McLachlin *et al.*, 1998). While a location of δ near the top of F_1 was clearly indicated by earlier work, the exact location has been controversial. Recently, a part of δ was localized to the dimple at the very top of F_1 by immunoelectronmicroscopy (Wilkens *et al.*, 2000) using a monoclonal anti-δ antibody. In addition, one view seen in the electron micrographs revealed an elongated region of protein density on the upper outside surface of F_1; this density could represent the C-terminal domain of *b* interacting with the C-terminal region of δ.

The possible dynamic nature of the interaction between the *b* and δ subunits was tested by linking them together through a disulfide formed between introduced cysteine residues (McLachlin and Dunn,

2000). Essentially complete disulfide formation, brought about by incubation of membranes containing this engineered ATP synthase with Cu^{2+}, had no effect on ATP-dependent proton pumping. This result demonstrates that *b*–δ interaction need not be dynamic and is probably static, in the normal, unlinked enzyme, consistent with the proposed role of $b_2\delta$ as a stator.

The interaction of *b* with δ is essential for F_1 and F_0 to bind together properly. However, the weakness of the interaction (reviewed by Dunn *et al.*, 2000b) suggests that additional contacts between b_2 and the $\alpha_3\beta_3$ hexamer of F_1 probably also contribute to binding. In a search for such sites, chemical crosslinks between cysteines introduced into the *b* subunit and the $\alpha_3\beta_3$ hexamer have been obtained and analyzed in our laboratory (McLachlin *et al.*, 2000). These studies utilized heterobifunctional reagents, such as *p*-azidophenacylbromide or benzophenone-4-maleimide, which react spontaneously with sulfhydryl groups at one end, and are photoactivatable at the other end. Cysteines introduced into b_{24-156} at positions 92 or 109 could be linked to α or β of F_1-ATPase and the linkages could be obtained in membrane-bound ATP synthase in which the same mutations had been introduced into the intact *b* subunit of the cysteineless ATP synthase encoded by pACWU1.2 (Kuo *et al.*, 1998). Analysis of the sites of linkage of b_{24-156} to F_1, carried out by peptide mapping and mass spectrometric analysis, showed that the cysteine in position 92 was linked to both α and β at sites near their respective C-termini. Based on the high-resolution structure of mitochondrial F_1, these peptides are located close to the lower edge of the $\alpha_3\beta_3$ hexamer, adjacent to one of the α/β interfaces which defines a noncatalytic nucleotide binding site. A significant feature was that in order to get the linkage from position 92 in membrane-bound enzyme, it was necessary to remove the F_1 from the F_0, modify the cysteine residue with the reagent, and then add the F_1 back, implying that the interaction of *b* with F_1 in this region is very tight and that parts of *b* may penetrate well into the cleft between the subunits. The likely position of a crosslink from cysteine in position 109 of b_{24-156} was within residues 213–220 of α, a region on the surface of the enzyme again close to an α/β interface containing a noncatalytic nucleotide binding site. In order to accommodate these results, the dimerization domain, modeled as a pair of helices, was positioned at an α/β interface such that residue 53 was about 40 Å below the lower surface of $\alpha_3\beta_3$ and residue 122 was 25–30 Å below the upper surface of $\alpha_3\beta_3$. This positioning would place the predicted bend of *b* (residues 80–84) in the deep cleft between the C-terminal helical domains of α and β.

Work in Rod Capaldi's laboratory showed that a disulfide bond could be formed between a cysteine introduced at the C-terminus of *b* and the naturally occurring Cys90 of one of the α subunits (Rodgers and Capaldi, 1998). The Cys90 site is located nearer the top of F_1 and closer to an α/β interface that contains a catalytic site. Together, these results could suggest that the path taken by *b* does not travel straight up toward the top of F_1, like a line of longitude on a globe, but has a lateral component as well. The crosslink to Cys90 was shown to inhibit ATP-driven proton pumping (Rodgers and Capaldi, 1998), indicating either that relative motion of *b* and α is essential, or else that formation of the crosslink distorted the enzyme to an inactive conformation.

Chemical cross-linking studies with yeast mitochondrial membranes have also indicated sites on subunit 4, the analog of *b* in yeast, that can be crosslinked to other subunits (Soubannier *et al.*, 1999). Of particular interest is position 174, thirty-five residues before the C-terminus, which can be linked to either β or OSCP, implying that it is near the interface of these two subunits.

DOES *b* HAVE A FUNCTION BEYOND CONNECTING F_1 AND F_0?

A number of years ago, evidence was obtained that the interaction of *b* with F_1 is essential not only for holding the complex together, but in triggering the maturation of F_0 to a proton-conducting form (Takeyama *et al.*, 1988; Angov *et al.*, 1991; Monticello and Brusilow, 1994). As yet, however, there is little evidence of the mechanism of this transformation.

The flexibility of *b* suggests a role, along with γε, in transiently storing energy during rotational catalysis. In the model developed by Wolfgang Junge and colleagues (Cherepanov *et al.*, 1999), these elements would undergo stepwise elastic deformation as protons moved through F_0. The energy would then be expended in one step to drive the conformational change allowing release of ATP from the catalytic site. In a different view, Oster and Wang (2000) have stressed the theoretical importance of *b* as a flexible, elastic link coupling F_1 and F_0 so that torque provided by either proton movement or ATP hydrolysis can be delivered more smoothly to the other component, resulting in

increased efficiency. In this model the amount of energy stored by the elastic element would be more nearly constant through the catalytic cycle. However, we are unaware of any direct evidence of whether the flexibility of *b* is elastic, as required in either of the above models, or inelastic. The suggested coiled-coil component of the dimerization domain offers a number of potentially elastic modes of deformation, including bending, stretching, and compression, although mechanisms involving electrostatic interactions between side chains are also conceivable.

Finally, recent studies from the laboratory of Pia Vogel and John Wise have shown that the soluble domain of *b* can influence the conformation of nucleotide-binding sites in F_1-ATPase (Kersten *et al.*, 2000). In these studies, a spin label was introduced at position β-331 in *E. coli* F_1-ATPase through use of a cysteine residue inserted by mutagenesis. The ESR spectrum of this spin label changed upon addition of b_{24-156} in a way implying that more of the catalytic sites were in an open conformation. This result shows the potential of *b* to influence catalytic events more directly than previously recognized and suggests that the coupling function of *b* may extend beyond the generally accepted linkage function.

ACKNOWLEDGMENTS

Work in the authors' laboratories was supported by Grants MT-10237 (to S.D.D.) and MT-15624 (to B.H.S.) from the Medical Research Council of Canada.

REFERENCES

Abrahams, J. P., Leslie, A. G. W., Lutter, R., and Walker, J. E. (1994). *Nature (London)* **370**, 621–628.
Angov, E., Ng, T. C. N., and Brusilow, W. S. A. (1991). *J. Bacteriol.* **173**, 407–411.
Blair, A., Ngo, L., Park, J., Paulsen, I. T., and Saier, M. H. (1996). *Microbiology* **142**, 17–32.
Boyer, P. D. (1997). *Annu. Rev. Biochem.* **66**, 717–749.
Caviston, T. L., Ketchum, C. J., Sorgen, P. L., Nakamoto, R. K., and Cain, B. D. (1998). *FEBS Lett.* **429**, 201–206.
Cherepanov, D. A., Mulkidhanian, A. Y., and Junge, W. (1999). *FEBS Lett.* **449**, 1–6.
Cipriano, D. J. and Dunn, S. D. (2000) unpublished observations.
Collinson, I. R., van Raaij, M. J., Runswick, M. J., Fearnley, I. M., Skehel, J. M., Orriss, G. L., Miroux, B., and Walker, J. E. (1994). *J. Mol. Biol.* **242**, 408–421.
Dmitriev, O., Jones, P. C., Jiang, W., and Fillingame, R. H. (1999). *J. Biol. Chem.* **274**, 15598–15604.
Dunn, S. D., unpublished observations.
Dunn, S. D. (1992). *J. Biol. Chem.* **267**, 7630–7636.
Dunn, S. D. and Chandler, J. (1998). *J. Biol. Chem.* **273**, 8646–8651.
Dunn, S. D., Bi, Y., and Revington, M. (2000a). *Biochim. Biophys. Acta*, **1459**, 521–527.
Dunn, S. D., Kellner, E., and Lill, H., manuscript submitted.
Dunn, S. D., McLachlin, D. T., and Revington, M. (2000b). *Biochim. Biophys. Acta* **1458**, 356–363.
Girvin, M. E., Rastogi, V. K., Abildgaard, F., Markley, J. L., and Fillingame, R. H. (1998). *Biochemistry* **37**, 8817–8824.
Greie, J.-C., Deckers-Hebestreit, G., and Altendorf, K. (2000). *Eur. J. Biochem.* **267**, 3040–3048.
Howitt, S. M., Rodgers, A. J. W., Jeffrey, P. D., and Cox, G. B. (1996). *J. Biol. Chem.* **271**, 7038–7042.
Kersten, M. V., Dunn, S. D., Wise, J. G., and Vogel, P. D. (2000). *Biochemistry* **39**, 3856–3860.
Kuo, P. H., Ketchum, C. J., and Nakamoto, R. K. (1998). *FEBS Lett.* **426**, 217–220.
Lau, S. Y. M., Taneja, A. K., and Hodges, R. S. (1984). *J. Biol. Chem.* **259**, 13253–13261.
McCormick, K. A., Deckers-Hebestreit, G., Altendorf, K., and Cain, B. D. (1993). *J. Biol. Chem.* **268**, 24683–24691.
McLachlin, D. T. and Dunn, S. D. (1997). *J. Biol. Chem.* **272**, 21233–21239.
McLachlin, D. T. and Dunn, S. D. (2000). *Biochemistry* **39**, 3486–3490.
McLachlin, D. T., Bestard, J. A., and Dunn, S. D. (1998). *J. Biol. Chem.* **273**, 15162–15168.
McLachlin, D. T., Coveny, A. M., Clark, S. M., and Dunn, S. D. (2000). *J. Biol. Chem.* **267**, 7630–7636.
Monticello, R. A. and Brusilow, W. S. A. (1994). *J. Bacteriol.* **176**, 1383–1389.
Nakamoto, R. K., Ketchum, C. J., and Al-Shawi, M. K. (1999). *Annu. Rev. Biophys. Biomol. Struct.* **28**, 205–234.
Oster, G. and Wang, H. (2000). *Biochim. Biophys. Acta* **1458**, 482–510.
Revington, M., Dunn, S. D., and Shaw, G. S., manuscript in preparation.
Revington, M., McLachlin, D. T., Shaw, G. S., and Dunn, S. D. (1999). *J. Biol. Chem.* **274**, 31094–31101.
Rodgers, A. J. W. and Capaldi, R. A. (1998). *J. Biol. Chem.* **273**, 29406–29410.
Rodgers, A. J. W., Wilkens, S., Aggeler, R., Morris, M. B., Howitt, S. M., and Capaldi, R. A. (1997). *J. Biol. Chem.* **272**, 31058–31064.
Sawada, K., Kuroda, N., Watanabe, H., Moritani-Otsuka, C., and Kanazawa, H. (1997). *J. Biol. Chem.* **272**, 30047–30053.
Shilton, B. H. and Dunn, S. D. (2000) unpublished observations.
Shilton, B. H., Revington, M., and Dunn, S. D. (1999) unpublished observations.
Sorgen, P. L., Bubb, M. R., McCormick, K. A., Edison, A. S., and Cain, B. D. (1998a). *Biochemistry* **37**, 923–932.
Sorgen, P. L., Caviston, T. L., Perry, R. C., and Cain, B. D. (1998b). *J. Biol. Chem.* **273**, 27873–27878.
Sorgen, P. L., Bubb, M. R., and Cain, B. D. (1999). *J. Biol Chem.* **274**, 36261–36266.
Soubannier, V., Rusconi, F., Vaillier, J., Arselin, G., Chaignepain, S., Graves, P.-V., Schmitter, J.-M., Zhang, J. L., Mueller, D., and Velours, J. (1999). *Biochemistry*, **38**, 15017–15024.
Stock, D., Leslie, A. G. W., and Walker, J. E. (1999). *Science* **286**, 1700–1705.
Takeyama, M., Noumi, T., Maeda, M., and Futai, M. (1988). *J. Biol. Chem.* **263**, 16106–16112.
Tiburzy, H. J. and Berzborn, R. J. (1997). *Z. Naturforsch* **52c**, 789–798.
Uhlin, U., Cox, G. B., and Guss, J. M. (1997). *Structure* **5**, 1219–1230.

Walker, J. E. (ed.) (2000). Special issue: The Mechanisms of F_1F_0-ATPase. Amsterdam: Elsevier Science, [290 pp.] (*Biochim. Biophys. Acta.* **1458**, Nos. 2–3).
Weber, J. and Senior, A. E. (1997). *Biochim. Biophys. Acta* **1319**, 19–58.
Wilkens, S., Dahlquist, F. W., McIntosh, L. P., Donaldson, L. W., and Capaldi, R. A. (1995). *Natur. Struct. Biol.* **2**, 961–967.
Wilkens, S., Dunn, S. D., Chandler, J., Dahlquist, F. W., and Capaldi, R. A. (1997). *Natur. Struct. Biol.* **4**, 198–201.
Wilkens, S., Zhou, J., Nakayama, R., Dunn, S. D., and Capaldi, R. A. (2000). *J. Mol. Biol.* **295**, 387–391.